



Michel, S., Dutertre, F., Denbow, M., Galan, C., & Briscoe, W. (2019). Facile Synthesis of Chitosan-Based Hydrogels and Microgels through Thiol-Ene Photoclick Crosslinking. *ACS Applied Bio Materials*.
<https://doi.org/10.1021/acsabm.9b00218>

Peer reviewed version

Link to published version (if available):
[10.1021/acsabm.9b00218](https://doi.org/10.1021/acsabm.9b00218)

[Link to publication record in Explore Bristol Research](#)
PDF-document

This is the author accepted manuscript (AAM). The final published version (version of record) is available online via ACS Publications at <https://pubs.acs.org/doi/10.1021/acsabm.9b00218>. Please refer to any applicable terms of use of the publisher.

University of Bristol - Explore Bristol Research

General rights

This document is made available in accordance with publisher policies. Please cite only the published version using the reference above. Full terms of use are available:
<http://www.bristol.ac.uk/red/research-policy/pure/user-guides/ebr-terms/>

Article

**Facile Synthesis of Chitosan-Based Hydrogels and
Microgels through Thiol-Ene Photoclick Crosslinking**

Sarah E.S. Michel, Fabien Dutertre, Mark L. Denbow, M. Carmen Galan, and Wuge H Briscoe

ACS Appl. Bio Mater., **Just Accepted Manuscript** • DOI: 10.1021/acsabm.9b00218 • Publication Date (Web): 02 Jul 2019Downloaded from <http://pubs.acs.org> on July 3, 2019**Just Accepted**

"Just Accepted" manuscripts have been peer-reviewed and accepted for publication. They are posted online prior to technical editing, formatting for publication and author proofing. The American Chemical Society provides "Just Accepted" as a service to the research community to expedite the dissemination of scientific material as soon as possible after acceptance. "Just Accepted" manuscripts appear in full in PDF format accompanied by an HTML abstract. "Just Accepted" manuscripts have been fully peer reviewed, but should not be considered the official version of record. They are citable by the Digital Object Identifier (DOI®). "Just Accepted" is an optional service offered to authors. Therefore, the "Just Accepted" Web site may not include all articles that will be published in the journal. After a manuscript is technically edited and formatted, it will be removed from the "Just Accepted" Web site and published as an ASAP article. Note that technical editing may introduce minor changes to the manuscript text and/or graphics which could affect content, and all legal disclaimers and ethical guidelines that apply to the journal pertain. ACS cannot be held responsible for errors or consequences arising from the use of information contained in these "Just Accepted" manuscripts.

Facile Synthesis of Chitosan-Based Hydrogels and Microgels through Thiol-Ene Photoclick Crosslinking

Sarah Michel[†], Fabien Dutertre^{†,‡}, Mark Denbow[§], M. Carmen Galan^{†}, and Wuge H.
Briscoe^{†*}.*

[†] School of Chemistry, University of Bristol, Cantock's Close, Bristol BS8 1TS, UK

[§] Fetal Medicine Unit, St Michael's Hospital, Southwell Street, Bristol BS2 8EG, UK

[‡] Current address: Univ Lyon, UJM-Saint-Etienne, CNRS, IMP UMR 5223, F-42023 Saint
Etienne, France

KEYWORDS: polysaccharide, microgel, chitosan, thiol-ene, nano-emulsion

ABSTRACT: Polysaccharide-based microgels are effective vectors for biopharmaceutics delivery and functional components in tissue engineering due to their bioactivity and biocompatibility. Currently, the synthesis of chemically crosslinked microgels typically requires long reaction times, high energy input and are low yielding due to low volumes of water phase used. Herein, we report the synthesis of norbornene-derivatized chitosan (CS-nbn-COOH), which can undergo rapid gelation in the presence of a thiolated crosslinker through the highly efficient thiol-ene photoclick reaction. This water-soluble photocrosslinkable derivative, synthesized on scale *via* a single step

from native chitosan and commercially available carbic anhydride, represents the first example of a norbornene-functionalised CS to the best of our knowledge. Microgels with controlled cross-linking densities and diameters varying between 100 and 400 nm were obtained via a low energy water-in-oil nano-emulsion templating method at room temperature, with photo-crosslinking initiated in a flow reactor powered with a domestic UV-A lamp, a method that is suitable for scale-up synthesis of the microgels. We also demonstrate that the resulting microgels were non-toxic to human dermofibroblasts (HDF) cell lines and that residual norbornene groups could be reacted in a late stage through tetrazine ligation, highlighting the potential of these microgels as scaffolds for functional nanomaterials with biomedical applications.

1. Introduction

Microgels consist of crosslinked polymer chains of dimensions ranging from 100 nm to hundreds of μm which can swell in a good solvent while retaining their initial three-dimensional structure.¹ These nanomaterials have been extensively exploited for the encapsulation and controlled release of drugs or biological molecules.²⁻⁴ In particular, polysaccharide-based materials are highly attractive in nanomedicine as they are non-toxic, abundant, and often bio-active due to their structural similarities with the extracellular matrix,⁴ and have therefore found applications in tissue engineering, drug delivery and biosensing.²⁻⁶

Chitosan (CS) is a polysaccharide derived from the partial deacetylation of chitin, comprised of α -(1 \rightarrow 4)-linked N-acetyl-D-glucosamine (GlcNAc) and β -(1 \rightarrow 4)-linked D-glucosamine (GlcN) repeating units.⁶ A key feature of CS is the presence of a free amine functional group that can be protonated, making it the only natural cationic polysaccharide⁶ which confers it with unique physicochemical properties^{6, 7} and antibacterial activity,⁸ and have therefore been extensively

studied in the area of waste water treatment,⁹ food packaging,¹⁰ cosmetics,¹¹ wound dressing,¹² tissue engineering,⁶ and drug delivery.^{7, 13} CS-based microgels are classically obtained from ionotropic crosslinking under basic pH¹⁴ or with sodium triphosphate, but their stability under physiological conditions can be challenging owing to the reversible nature of these interactions.¹⁵ Covalent microgels have therefore been developed by chemical crosslinking of the backbone amines with glutaraldehyde¹³ or genipin.¹⁷ Reactions using these crosslinkers, however, present limited chemical selectivity which tend to produce side-products that often remain encapsulated within the microgels and potentially lead to cytotoxicity once used *in vivo*.¹³ Moreover, the exact crosslinking mechanism remains unclear, with both crosslinkers known to potentially polymerize, giving little control over the final structure of the micro-/nanogel.^{18, 19}

To allow more selectivity and hence better control over the crosslinking density and microgel structure, CS can be functionalised with a reactive group that could be activated with the appropriate chemical partner for hydrogel formation. In particular, click chemistry, a term often coined for high yielding, biorthogonal reactions that proceed even at low concentrations of reactive groups, has now become common in material chemistry, especially for biomedical applications.²⁰ In this context, the reaction between thiols and alkenes through the Michael addition or radical photoinitiated thiol-ene coupling are widely used. CS precursors activated in this manner are typically obtained by acrylation, which are susceptible to polymerisation under thiol-ene conditions.^{21, 22} To prevent dimerization, while allowing for spatio-temporal control through photoinitiation, norbornene (nbn) has been used in the radical thiol-ene conjugation.²¹⁻²³ The very fast kinetics of this addition and its feasibility with long-wavelength UV-A coupled to the use of photoinitiator Irgacure 2959 (PI) has made this thiol-ene reaction ideal in tissue engineering application.²¹ In addition, norbornene is stable *in vivo*²⁴ and can undergo orthogonal click reactions

with tetrazines, which allows for sequential functionalisation of materials.²⁵ While thiol-ene photoclick-generated hydrogels from norbornene-functionalised biopolymers such as gelatin,²⁶ alginate,²⁷ carboxymethyl cellulose²⁸ or hyaluronic acid²⁹ have been synthesized, CS-derived hydrogels or microgels using norbornene-mediated thiol-ene photoclicking have not been reported previously. We note that photocrosslinked hydrogels using maleimide-³⁰, azido- or (meth)acrylate-functionalised CS have been reported;²² however, this has not been extended to photocrosslinked microgels.

Nano-emulsion-templated methods are commonly used for precise control over the microgel size. Typically, an aqueous polymer solution (the dispersed phase) is added dropwise into a non-miscible oil phase (the continuous phase) containing surfactants to generate nano-sized water droplets. The crosslinking is then performed in these nanoreactors to give monodisperse nano-/microgels. There are a few examples of click nano-/microgels obtained by nano-emulsions, especially concerning polysaccharide materials. Jia *et al.* reported hyaluronic acid (HA)-based microgels obtained by reacting a hydrazide- and aldehyde-functionalised polymers in a reverse nano-emulsion template,³¹ while Anderson *et al.* chose dextran complementarily derivatised with alkynes or azides beforehand.³² Dilute concentrations of the nano-emulsion droplets and requirement for shearing or sonication limit the suitability of this method for scale-up or fragile biomolecules.³³ Recently, Gupta *et al.* reported a concentrated nano-emulsion system in decane with the droplets stabilised by FDA-approved surfactants Span[®] 80 (S80) and Tween[®] 80 (T80), using a low-energy homogenisation which was successfully applied to the synthesis of calcium-based alginate microgels.³³

We report herein the synthesis and characterisation of CS-based microgels obtained through photo-mediated thiol-ene crosslinking (**Figure 1**) using a nano-emulsion templated protocol.

Norbornene moieties were incorporated to CS through amide bond formation using commercially available carbic anhydride (CA). The carboxylate groups introduced in this manner further enhanced solubility of CS in aqueous media. Gelation was demonstrated by crosslinking of the resulting derivative CS-nbn-COOH with a short bifunctional thiolated-diethylene glycol crosslinker (HS-DEG-SH). A concentrated water-in-oil nano-emulsion was developed and optimised in terms of the oil type and surfactant composition, which was successfully applied to the synthesis of CS microgels using a custom-designed photoreactor. The accessibility of pendant reactive groups subsequent to gelation for functionalisation was demonstrated by fluorescence through tetrazine conjugation using a self-quenching probe, further demonstrating the potential of these microgels as building units for functional materials. Finally, the microgels did not present any significant toxicity against human dermofibroblast (HDF) cell lines, which suggests their possible biomedical applications.

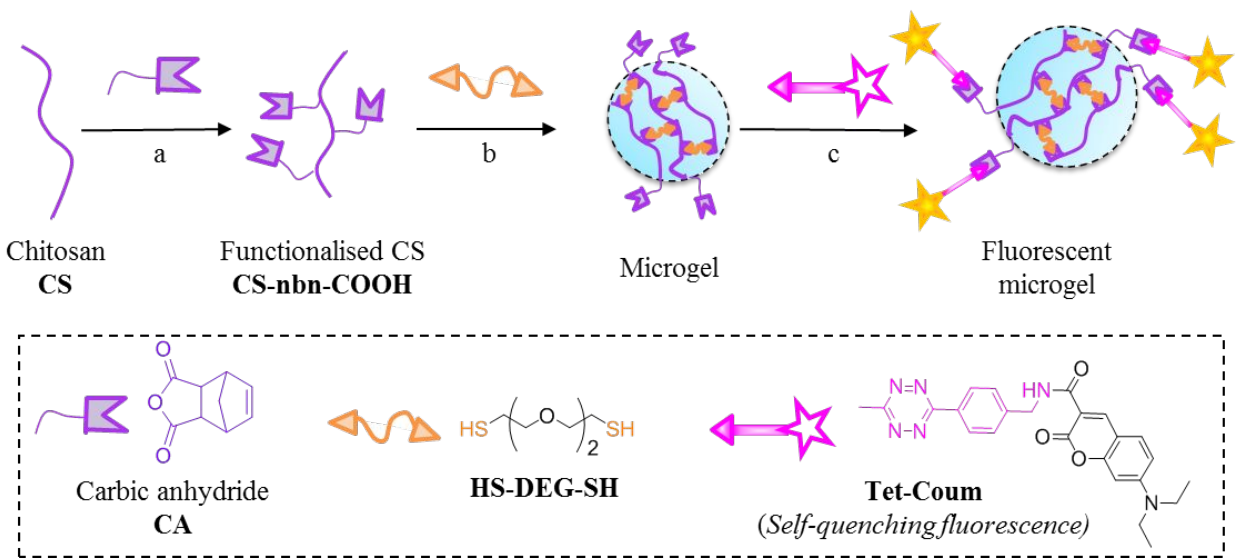


Figure 1. Schematic representation of the functionalised microgel synthesis. (a) Chitosan (CS) was first reacted with carbic anhydride (CA) to give CS-nbn-COOH. (b) Microgels could be successfully obtained by crosslinking CS-nbn-COOH with a thiolated crosslinker, HS-DEG-SH,

using a nano-emulsion-templated method in the presence of UV-A and Irgacure 2959 (PI) as a photoinitiator. (c) The reactivity of remaining norbornene groups present on the microgels was proven by fluorescence using a self-quenching tetrazine, Tet-Coum.

2. Materials and Methods

The chemical structures of the reagents used are listed in **Figure S1** in the ESI. Chitosan (CS, low molecular weight 50-190 kDa, deacetylation degree = 76 % calculated by ^1H NMR – see **Figure S2** in the supporting information section **SI-II**) was purchased from Sigma. Carbic anhydride (CA, mixture of *endo* and *exo* predominantly *endo*) was purchased from Acros. 7-(diethylamino)-N-(4-(6-methyl-1,2,4,5-tetrazin-3-yl)benzyl)-2-oxo-2H-chromene-3-carboxamide (Tet-Coum) was synthesized according to previously described procedures as detailed in the ESI in section **SI-X**. Other reagents were purchased from Sigma, Acros, Fluka or Lancaster and used as received. All cell culture media and additives were purchased from Invitrogen, Life Technologies (Thermo-Fisher). Dialysis against dionised (DI) water (MilliQ; resistivity 18.2 M Ω cm and total organic content (TOC) < 4 ppb) were performed using a SnakeSkin dialysing tubing with a molecular weight cut-off (MWCO) of 10 kDa (Thermo Scientific).

^1H NMR were recorded with a Varian VNMR S600 Cryo at 40 °C to sharpen the water peak and to allow for more accurate integration of the norbornene peaks. CS polymer samples were prepared in 1 % DCl/D $_2\text{O}$ whereas the microgels were resuspended in D $_2\text{O}$ only. UV-mediated photoclick reactions were performed with a 36 W UV-A lamp (320-400 nm) of domestic use (PL-L, approximative length 30 cm, Philips).

2.1. Synthesis of CS-nbn-COOH

CS (1 g, 5.9 mmol) was dissolved in 100 mL of 2% acetic acid (AcOH) in DI water. Once solubilised, carbic anhydride (CA, 972 mg, 5.9 mmol) was added, and the mixture was stirred at

50 °C for 2 days. The resulting polymer conjugates were dialysed against 5% NaCl for 24 hrs followed by dialysis in DI water for 2 further days, and then lyophilised. Effective removal of unreacted CA was verified by DOSY NMR (**Figure S3**), and the degree of substitution (DS) was calculated by ^1H NMR as detailed in **Figure S4**.

2.2. Optimisation of the synthesis of CS-nbn-COOH by experimental design

Experimental DS design of CS was performed using MODDE 9.1 software. Three parameters were studied: temperature (varied between 25 and 50 °C), reaction time (6 to 48 hrs), and equivalents of carbic anhydride (0.5 to 1.5). DS was chosen as the only variable to measure the result; the desired value was set to 50%. 11 experiments were suggested by the software (**Table S1**), which were conducted with 50 mg of CS in 5 mL of a 2% AcOH solution. The reaction was carried out as described in Section 2.1 and the experimental analysis was performed with MODDE 9.1 using a standard screening design.

2.3. Hydrogel synthesis

To assess the gelation feasibility and optimise gelation conditions for microgels, hydrogels of CS-nbn-COOH were first prepared. CS-nbn-COOH was dissolved in a 0.1% solution of photoinitiator Irgacure 2959 (PI) in 2% AcOH to the desired concentration, varied between 0.5 and 2 w:v%. Once soluble, the thiolated crosslinker 2,2'-(Ethylenedioxy)diethanethiol (HS-DEG-SH) was added to give a thiol:norbornene [SH]:[nbn] molar ratio R_s varying between 25 ($R_s = 1:4$) and 100% ($R_s = 1:1$) of reacted norbornene groups. The mixture was transferred in a sealed glass vial (dimensions: $l = 36\text{mm}$, $d_{outer} = 11\text{ mm}$), vortexed and cured by direct exposure on top of a UV-A lamp (distance lamp – sample $\sim 0\text{ mm}$). The UV time exposure was varied between 20 sec to 30 min. Hydrogel formation was assessed by the vial-inverted method as described below. At the desired time-scale, the sample curing was stopped, and the sample was inverted. If the material

flowed the curing was prolonged for a desired period of time. The sample was finally inverted overnight and was called “gel” if a set material was obtained after 16hrs or “viscous liquid” if not.

2.4. Rheology

Rheological measurements on the obtained hydrogels were performed with a Kinexus rheometer using a parallel plate geometry P20 ($d = 20$ mm) and a Peltier system for temperature control. The gel samples were synthesized in a 3D-printed PLA mould (diameter 21.5 mm, height 5.9 mm volume ~ 2.1 mL) partially filled with 800 μL of a pre-mixed solution of polymer (10 mg/mL), PI (1 mg/mL) and the HS-DEG-SH crosslinker to vary R_s between 1:4 and 1:1, all solubilized in 2% AcOH. Samples were cured without preliminary degasing with a UV-A lamp (distance lamp – sample = 5 mm) for 30 min to ensure complete crosslinking. Hydrogels were carefully loaded on the rheometer and equilibrated with a normal force of 0.1 N (typical gap 1.7-2 mm). Dynamic strain sweeps were performed at 1 Hz by varying the strain γ from 0.1 to 100 % at 25 °C. All measurements were performed in triplicates. A temperature cartridge was used to prevent solvent evaporation during measurement.

2.5. Nano-emulsion preparation and characterisation

The nano-emulsions were prepared according to the procedure described by Gupta *et al.*³³ They were composed of 80 wt% of oil, 10 wt% of surfactants (Span[®] 80 (S80) and Tween[®] 80 (T80) in weight ratios varying between 20 and 100% of S80) and 10 wt% of the water phase, consisting of either DI water or 1 w:v% CS or CS-nbn-COOH in 2% AcOH. Three oils were screened: decane which allowed a comparison with published results,³³ cyclohexane which had a similar viscosity to decane but a lower boiling point thus making its removal easier, and mineral oil which is biocompatible and FDA-approved. S80 and T80 were chosen as they are widely used in biomedical applications; they are also neutral, which was expected to minimise the electrostatic interactions

with the charged CS. The water phase was added dropwise to a stirred solution of surfactants in the desired oil phase at 700 rpm. The nano-emulsion was stirred for at least 10 min. DLS measurements were performed using a Malvern Nano Zetasizer zs with a 633 nm laser, immediately after dilution of 100 μ L of the nano-emulsion into 900 μ L of oil to avoid multi-scattering from concentrated and turbid nano-emulsions in a glass cuvette. Autocorrelation functions were measured at a scattering angle of 173° at 25 °C and processed using the Malvern software package.

2.6. Microgel synthesis

Microgels were obtained using the nano-emulsion templating method described above, where the water phase consisted in 1% w:v CS-nbn-COOH solution in 0.1 % w:v PI in 2 % AcOH to which was added the crosslinker HS-DEG-SH to give R_s varying between 1:4 and 1:1. The nano-emulsion was crosslinked in flow using the device developed by Booker-Milburn *et al.*³⁴ (For full details on the set-up see section SI-VII in ESI). Briefly, the nano-emulsion was pumped through a UV-permeable tubing wrapped around a domestic UV-A lamp. The flow rate r could be tuned to vary the crosslinking time between 4 and 15 min. The crosslinked microgels were collected at the end of the device (**Figure 2**) and recovered by centrifugation at 7000 rpm for 3 hrs at 6 °C. The organic layer was decanted and the microgels were subsequently washed with ethanol and DI water sequentially, and then lyophilised. The microgels were resuspended in DI water ($c \sim 0.5$ to 1 mg/mL) and their hydrodynamic diameter d_h and Zeta potential ξ were both measured with a Zetasizer as described in section 2.5.

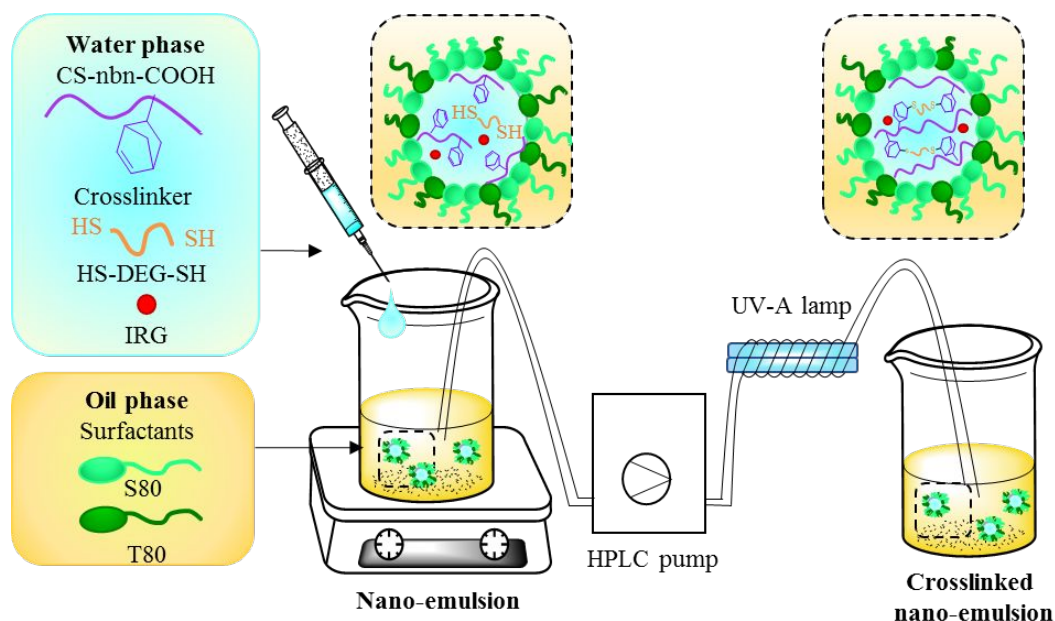


Figure 2. Synthesis of crosslinked microgels in flow using UV. A simple HPLC pump is used to pump the nano-emulsion through the EPF tubing, which is wrapped around a domestic UV-A lamp. The exposure time is readily tuned between 1-30 min by varying the flow rate. The nano-emulsion used for these tests was made of 80 wt% cyclohexane, 4 wt% S80, 6 wt% T 80 and 10% wt of water phase (1% CS in 2% AcOH).

2.7. TEM imaging

The samples were prepared by negative stain using uranyl acetate (3 %) on glow discharged grids. 5 μ L of microgel suspensions (0.5-1 mg/mL) was incubated on the grid for 1 min and the excess was wicked away; the procedure was then repeated with 5 μ L of stain. The samples were observed in a Tecnai 12 BioTwin TEM at 120 kV with images captured using an FEI Eagle 4k \times 4k camera.

2.8. Microgel functionalisation

The microgels ($R_s = 1:2$) were resuspended in DI water at a final concentration of final concentration of 0.5 mg/mL in a quartz cuvette (1 cm pathlength) to which Tet-Coum was added to a final concentration of 1 μ M. The ratio between unreacted norbornene and Tet-Coum was 1:1,

assuming 100% yield for the thiol-ene crosslinking in the microgel synthesis step. The reaction was monitored by fluorescence spectroscopy using a Perkin-Elmer LS45 fluorimeter with an excitation at 420 nm. The emission spectra were recorded in the wavelength range of 460 - 600 nm.

2.9. Cytotoxicity assays

HDF cells were maintained in Dulbecco's Minimal Essential Medium (DMEM) with 1g glucose/L, GlutaMAX™ and 10% fetal bovine serum (FBS) supplemented with antibiotic-antimycotic (AntiAnti). Confluent cultures were detached from the surface using trypsin (Tryp LE Express) and plated at 5×10^3 cells/well in 96-well plates. The cells were incubated 24 h after plating with microgels ($R_s = 1:1$) at concentrations varied between 1000 and 2 $\mu\text{g/mL}$ (4 replicates per condition, *i.e.* toxicant concentration and time point, all performed in triplicates) for 1 or 2 days. At the required incubation time, the medium was removed and wells were rinsed twice with phosphate buffer saline (PBS). Metabolic activity and cell viability were measured by feeding the cells with FBS-free medium containing 5% Alamar Blue (AB, metabolic activity) and 3 μM Calcein AM (cell viability) for 1 h. Fluorescence was recorded with a CLARIOstar plate reader (AB: excitation 515-555 nm, emission 510-530 nm; Calcein AM: excitation 414-483, emission 510-530 nm). All results were background-corrected with a solution of media containing the two dyes and expressed as a percentage of control consisting of cells not exposed to microgels.

3. Results and Discussion

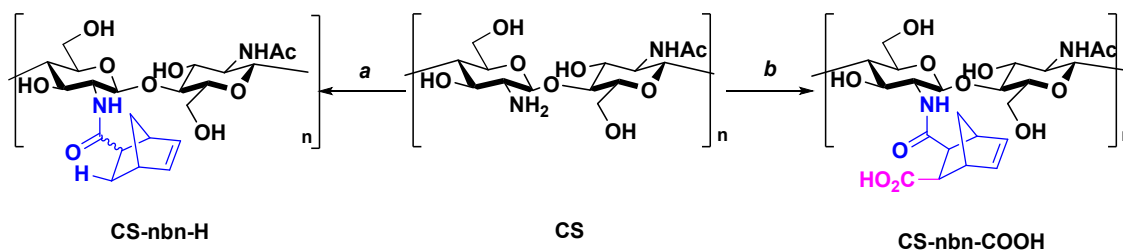
3.1. Synthesis and characterisation of norbornene-functionalised chitosan (CS-nbn-H and CS-nbn-COOH)

Amide bonds are commonly used to functionalise CS by exploiting the higher nucleophilicity of the amines compared to hydroxyl groups. CS amidation with norbornene-carboxylic acid (NB)

using 1, 1'-carbonyldiimidazole (CDI) resulted in the successful synthesis of CS-nbn-H (**Scheme 1** route a) as evidenced by ^1H NMR (**Figures S5** and **S6**). It is noteworthy that amide coupling using 1-ethyl-3-(3-dimethylaminopropyl)carbodiimide (EDC) and N-hydroxysuccinimide (NHS)-activated NB led to mixtures of product and unreacted EDC that could not be separated by dialysis or precipitation (see section **SI-III** for details on the purification procedures attempted).

CS-nbn-H suffered from low solubility even under acidic conditions or in the presence of different solubilizing reagents and/or co-solvents (**SI-III**), which is probably due to the reduction of the positive charge as CS amines were converted to amides, in combination to the increased overall hydrophobicity induced by the addition of NB groups.

To circumvent this, carbic anhydride (CA) was used to react with the CS amine groups, which upon ring opening resulted in the concomitant amide formation and introduction of an acid functionality on the pendant norbornene that led to the polymer CS-nbn-COOH (**Scheme 1**, route b). Compared to CS-nbn-H, CS-nbn-COOH was soluble not only in mild acidic conditions, but also in DI water, which likely results from both the introduction of a carboxylic acid group and by the concomitant disruption of the hydrogen bond network as amines react, as previously reported.³⁵



Scheme 1. Strategies to obtain norbornene-functionalised CS. Reaction conditions: a) norbornene-2-carboxylic acid (NB), CDI, 0.1 M MES buffer pH 5.0. b) carbic anhydride (CA), 2% AcOH.

As summarised in **Table S1**, an increase in the degree of substitution (DS) of the amines by norbornenes was observed as the reaction time, the temperature, or the equivalent of CA increased,

1
2
3
4
5
6
7
8
9
10
11
12
13
14
15
16
17
18
19
20
21
22
23
24
25
26
27
28
29
30
31
32
33
34
35
36
37
38
39
40
41
42
43
44
45
46
47
48
49
50
51
52
53
54
55
56
57
58
59
60

varying between 24 and 43%. **Figure 3** shows that the reaction time and the amount of CA significantly contributed to the DS (**A**), whilst the temperature and the reaction time in conjunction had less impact on the final DS, as suggested by the dominant green color (**B**). Hence, the most efficient way to increase the DS is to increase the amount of CA and/or to increase the reaction time, rather than varying the temperature. This short screening showed that the reaction was reproducible and allowed for the generation of a reliable model ($q^2 = 0.365$, $r^2 = 0.924$). This DS is consistent with values reported for gelatin functionalisation with CA under similar conditions, where pH and norbornene steric hindrance were identified as the main limitation.^{26, 36} McOscar and Gramlich in particular showed that the reaction was highly pH-sensitive, with an optimum functionalisation occurring in the pH window 9.0-10.5, attributed to the balance between nucleophilicity of the carboxylate and the competitive hydrolysis of CA, both favoured at basic pHs.²⁸ As the CS solubility required initial mild acidic conditions, pH could not be used as a variable, and the synthesis of CS-nbn-COOH was further conducted for 48 hrs with 1 equivalent of CA at 50 °C to improve its solubility, which yielded a DS of 38%.

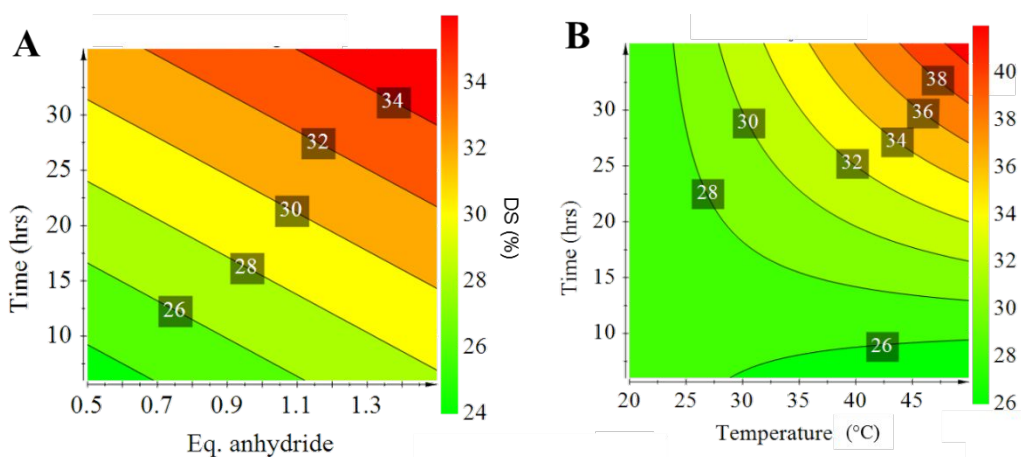
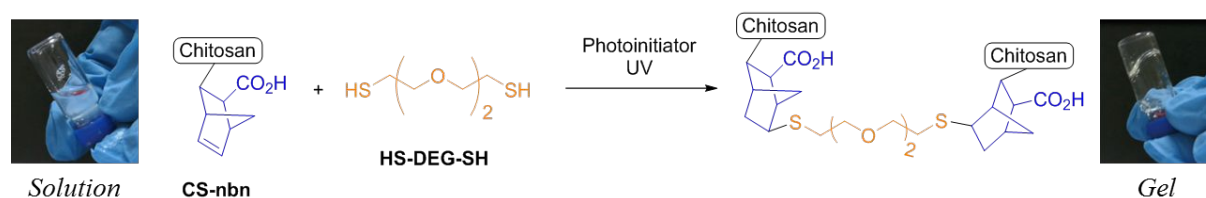


Figure 3. Contour plots showing the effect of the reaction time and the equivalents of CA **2** at 35 °C (**A**) and of the temperature and reaction time for 1 eq. of CA used (**B**) on the DS of CS-nbn-COOH. Degree of substitution (DS shown in mol%) obtained for a matching set of conditions,

where the impact of a set of parameters on the final DS is shown by a change from green (low) to red (high).

3.2. Hydrogel synthesis

The optimum gelation conditions of CS-nbn-COOH were screened for the subsequent microgel synthesis. The bifunctional crosslinker, 2,2'-(ethylenedioxy)diethanethiol (HS-DEG-SH, **Scheme 2**), was chosen due to its hydrophilicity and its flexibility compared to other small difunctional thiols such as dithiothreitol (DTT), frequently used in thiol-ene crosslinkings.^{26, 37, 38} Compared to longer thiolated PEGs, it is cost effective and readily available. The crosslinking was performed in the presence of Irgacure 2959 (PI, 0.1 w:v%) as the water-soluble photoinitiator. Different polymer and crosslinker concentrations were tested and gelation was assessed by the inverted vial method (**Figure 4**). At 0.5% polymer concentration, the viscosity of the dispersion increased progressively as the [SH]:[nbn] molar ratio, R_s , increased from 1:4 to 1:1 (**Figure S7A**). However, no gelation occurred even when the UV exposure was prolonged to 1 hr. For polymer concentrations of 1 and 2%, gels were formed instantly when the CS-nbn-COOH solution was exposed to UV light even for $R_s = 1:4$ (**Figure S7B and S7C**). The completion of the reaction was confirmed by *in situ* ^1H NMR, evident from the disappearance of the norbornene peaks at 6.2 ppm (**Figure S8B and S8C**).



Scheme 2. Reaction scheme of the thiol-ene cross-coupling reaction used for the hydrogel synthesis.

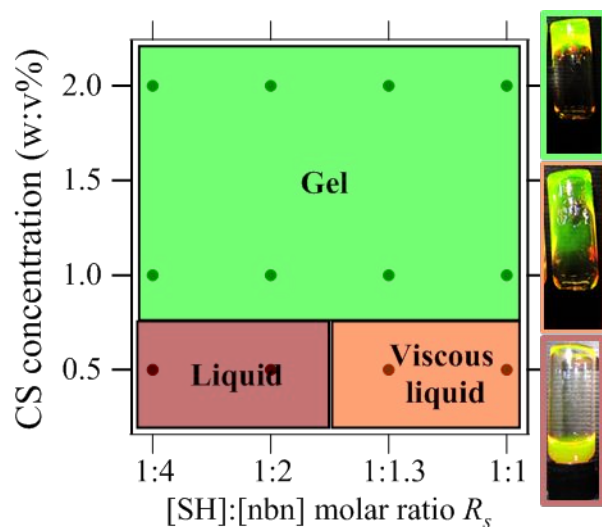


Figure 4. Gel phase diagram of CS-nbn-COOH depending on the polymer concentration and the [SH]:[nbn] molar ratio R_s . The curing was performed with UV-A for a duration of 20 sec to 30 min; at polymer concentrations > 1 % gelation occurred instantly. Example of a stained samples corresponding to the observed phases (liquid, viscous liquid and gel) are shown on the side, with further photos for all conditions presented in **Figure S7**.

Such fast gelation kinetics has been previously reported when norbornene was used as the alkene component in the thiol-ene click reaction. For instance, Lee *et al.* measured the gelation kinetics of a tetra-arm, norbornene-functionalised PEG with thiolated carboxymethylcellulose by photorheology. They found that gelation occurred within 5 sec, independently of the thiol content.³⁹ McOscar and Gramlich also worked with carboxymethylcellulose and the same HS-DEG-SH crosslinker, and reported that crosslinking was mostly complete within 15 sec.²⁸ In comparison, Hachet *et al.* have previously reported dextran⁴⁰ and HA-based hydrogels and nanogels resulting from the thiol-ene reaction between the pentenoic side chains of the polysaccharide and a thiolated PEG crosslinker.⁴¹ Gelation occurred in 2.5 min for the fastest systems, and up to 20 min for the longest. As their polysaccharide system and DS compare well

with ours, this difference in the reaction kinetics most likely arises from their terminal alkene choice, which is less reactive than norbornene. Overall, our results compare well with literature.

3.3. Rheology measurements of hydrogels

The rheological properties of the obtained hydrogels using 1 % CS-nbn-COOH were analysed with amplitude sweep measurements at 1 Hz. For all the [SH]:[nbn] ratios studied ($R_s = 1:4$ to 1:1), the storage modulus G' was ~ 10 times higher than the loss modulus G'' which corresponds to a solid behaviour at this frequency, characteristic of an elastic or gel-like material. Both G' and G'' were constant up to a critical strain $\gamma_c = 10$ % which defines the linear response of this hydrogel (**Figure 5A**). As R_s increased, G' increased from around 30 to 200 Pa, confirming an increase in the crosslinking density. Similar results were obtained by Gramlich *et al.* from norbornene-functionalised hyaluronic acid crosslinked with DTT, where the compressive modulus increased linearly with R_s .³⁷ On the other hand, McOscar and Gramlich reported near identical hydrogel mechanical properties for $R_s = 1:1$ and $R_s = 1:2$, which they attributed to a chain immobilisation effect preventing further crosslinking points to be made.²⁸ The polymer concentration in our system was much lower (10 mg/mL compared to their 40 mg/mL) which would allow for greater chain mobilities, consistent with the modulus of our hydrogels which was ~ 3 orders of magnitude smaller than that reported by McOscar and Gramlich. A greater range of elastic modulus could be realised by varying the polymer and crosslinker concentration, currently under investigation.

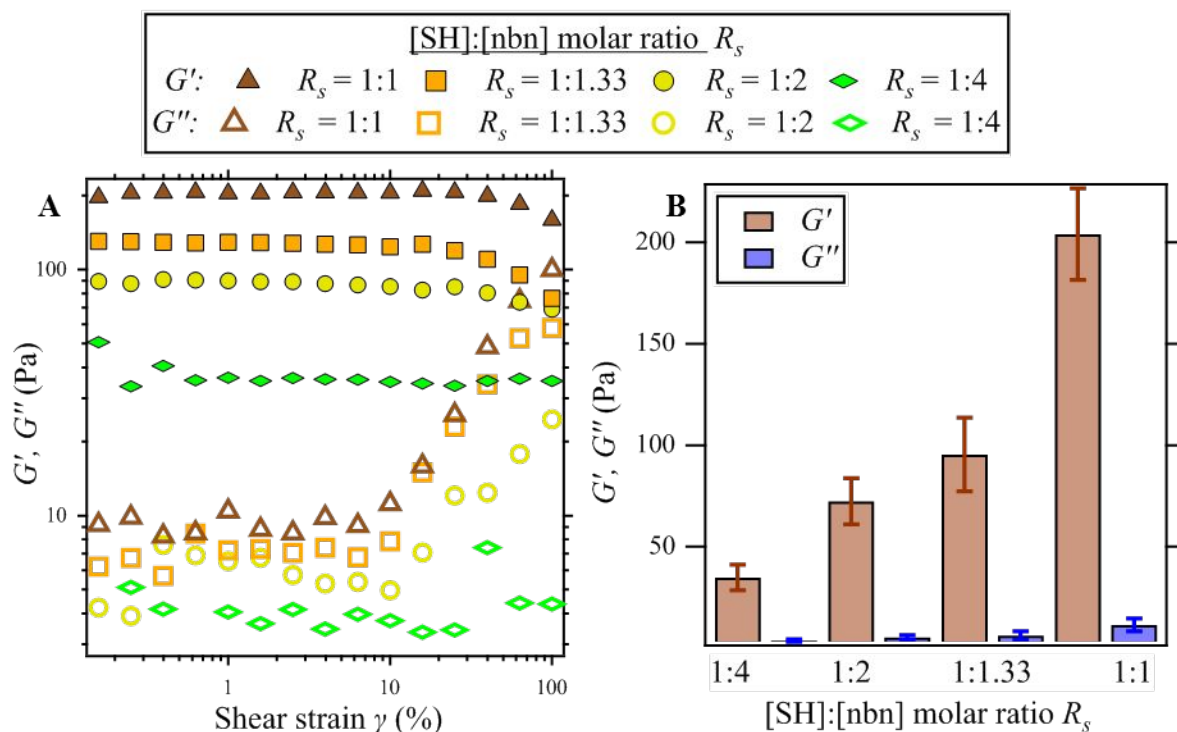


Figure 5. Rheological properties of the CS-nbn-COOH hydrogels. A) Variation of G' and G'' with the shear strain γ , at different [SH]:[nbn] molar ratios R_s ; B) Variation of G' and G'' with R_s , averaged on the linear response plateau value. Measurements were repeated in triplicates.

3.4. Optimisation of microgel formation

We focused on a low energy methodology developed by Gupta *et al.*³³ to generate concentrated nano-emulsions, using a system made of 80 wt% of oil 10 wt% of surfactants (S80 and T80) and 10 wt% of water. The impact of the oil type and the surfactant composition on the nano-emulsion stability was first investigated with surfactant compositions varying between $\nu = 1:0$ to 3:7 weight ratios of S80/T80 (**Figure 6**). As T80 was added to the cyclohexane or decane nano-emulsions, the turbidity decreased, transforming from white cloudy suspensions ($\nu = 1:0$ to 6:4 for cyclohexane, **Figure 6A**, and 1:0 to 7:3 for decane, **Figure 6B**, respectively) progressively to pale

blue ($\nu = 1:1$ and $6:4$, respectively for cyclohexane and decane), and to a transparent suspension ($\nu = 4:6$ and $1:1$, respectively for cyclohexane and decane, indicated by dashed rectangles on **Figure 6**), after which a pale blue colour was obtained. For the S80:T80 ratio higher than $\nu = 3:7$, phase separation occurred as soon as the stirring was stopped. These visual observations correlated with the hydrodynamic radius d_h measured by DLS (**Figure 6D**), which decreased from $d_h \sim 150$ - 200 nm down to $d_h \sim 40$ nm when the nano-emulsion was optically transparent, and then increased slightly as the turbidity increased again.

These observations agreed with previous work by Robin *et al.* performed in cyclohexane, where aggregates of ~ 150 - 200 nm were observed when only S80 was used, while the nano-emulsion turbidity decreased with the addition of T80; in addition, d_h decreased from ~ 100 to ~ 40 nm. No stable nano-emulsion could be generated when only T80 was used. Although we did observe that the mixtures of S80 and T80 generated more stable nano-emulsions with smaller diameters, a linear relationship between the dispersion turbidity and their hydrodynamic diameter could not be established. Robin *et al.* also reported that S80/T80 mixtures in cyclohexane could lead to both spherical and sheet-like morphologies depending on the concentration range, which may account for these discrepancies.⁴²

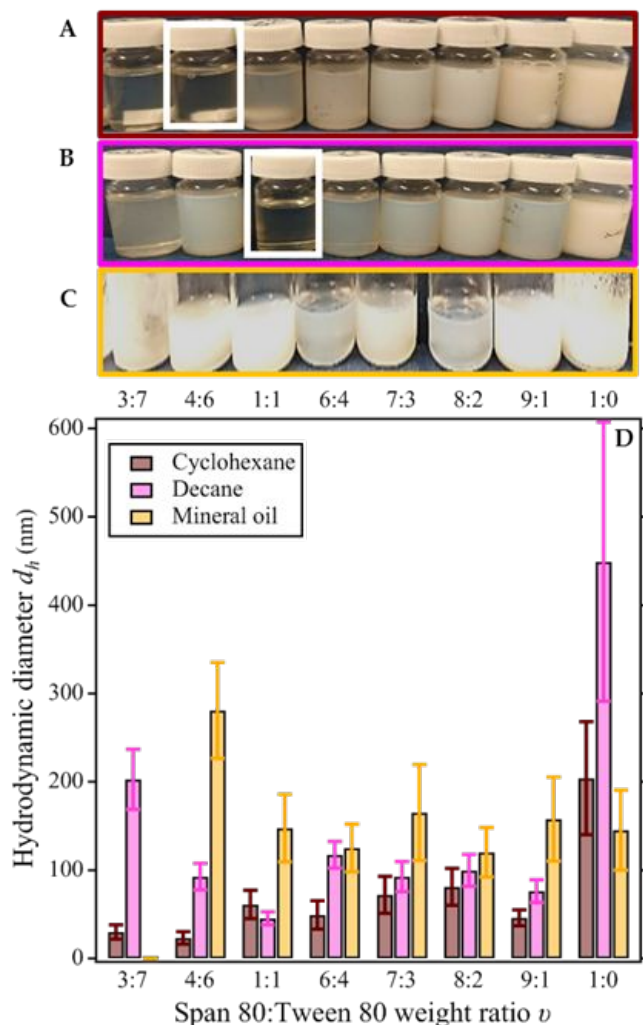


Figure 6. Visual observations of control nano-emulsions generated with: **A)** cyclohexane (brown), **B)** decane (pink), **C)** mineral oil (orange) for different surfactants ratios ν , and **D)** the corresponding hydrodynamic diameter d_h measured by DLS. Optimum nano-emulsion formulation was obtained for cyclohexane and decane consisted respectively of $\nu = 4:6$ and $\nu = 1:1$ (white rectangles in **A** and **B**).

While both cyclohexane and decane allowed for the formation of translucent nano-emulsions at low S80 weight ratio which remained stable over 2 months, emulsions formulated in mineral oils showed a different behavior. No optically clear emulsion could be obtained, and phase-separation occurred between several min and up to 5 hrs as the stirring was stopped. While milky

emulsions were observed for $\nu = 1:0$ to $9:1$, further increasing T80 decreased the nano-emulsion turbidity from white to pale blue up to $\nu = 4:6$, after which the turbidity increased again. At $\nu > 2:8$, no stable emulsions could be generated (**Figure 6C**). This was accompanied by d_h decreasing from ~ 150 to ~ 100 nm and increasing to ~ 300 nm for $\nu > 6:4$ (**Figure 6D**).

The diameter of nano-emulsion droplets has been shown to be highly dependent on the viscosity of both the continuous and the dispersed phases as well as the homogenisation procedure. For instance, Grupta *et al.* developed a scaling parameter $We_{crit, d}$ to predict the nano-emulsion droplet size based on these three parameters and successfully applied it to several oil-in-water nano-emulsions. They found that nano-emulsion droplet decreased with an increase in the continuous phase viscosity μ_c according to $d_h \sim \mu_c^{-5/12}$ – and therefore smaller droplet would be expected with mineral oil.⁴³ It is worth noting that the model was valid in a viscous turbulent regime, which also typically required high-energy homogenisation such as high pressure homogenisation or ultrasonication.⁴⁴ Our work, however, used as we used reverse nano-emulsions and also focused a low-energy mixing procedure. We suggest that this low energy emulsification methodology would not sufficiently disperse the water droplets in the continuous phase, leading to the phase-separation as observed.

All these elements, *i.e.* turbidity, low-stability, and $d_h > 100$ nm, strongly indicate that the mineral oil led to the formation of emulsions while cyclohexane and decane both gave stable nano-emulsions. We thus did not further pursue using mineral oil.

As a control, the effect of adding CS and CS-nbn-COOH to the water phase on both the size and the stability of the nano-emulsion droplets was also studied, given the cationic weak polyelectrolyte nature of CS and the hydrophobic character of norbornene. As lower viscosities of the dispersed phase have been shown to favour nano-emulsion stability, we focused on a CS

concentration of 1 w:v% in 2% AcOH, which was the lowest viscosity we could reach while allowing for gelation.⁴³ When either CS or CS-nbn was used as the water phase, the diameter of the resulting nano-emulsion droplets was largely the same, with a minimum diameter observed for the same optimal surfactant composition in both decane ($\nu = 1:1$ (**Figure S9**) and cyclohexane ($\nu = 4:6$; **Figure S10**), confirming the feasibility of using these nano-emulsions as template to generate microgels. Interestingly, several studies have reported the use of these surfactants at ratios which we show here were unfavourable ($\nu = 1:0$ ³² or $\nu = 8:2$ ^{38, 45}).

3.5. Optimisation of the conditions for the crosslinking of microgels in flow

To ensure efficient and complete photo-crosslinking, adequate UV illumination is usually facilitated either by long exposure time or expensive, high power light source. Here we have used a simple flow chemistry reactor made of FEP tubing wrapped around a domestic UV-A lamp (see **Figure 2**).³⁴ This method allowed for an optimal and homogeneous exposure of the nano-emulsion to the UV light, as it was pumped through the tubing. In addition, the crosslinking time could be tuned between 1 and 30 min by varying the flow rate. Using the optimised nano-emulsion conditions in this set-up, we investigated the feasibility of microgel crosslinking in flow by gauging the nano-emulsion stability with DLS after pumping and UV exposure at different pump rates r (**Table S2**).

A minimum of $r = 150$ rpm was required to maintain nano-emulsion stability during pumping and UV exposure, as demonstrated by DLS measurements of the nano-emulsion at the entrance and at the exit of the flow reactor (**Table S2**). Slower reactions ($r = 100$ rpm) resulted in droplet coalescence, as shown by both an increase in the nano-emulsion turbidity and by an increase in the hydrodynamic diameter d_h from ~ 30 nm to ~ 70 nm. At $r = 50$ rpm CS was visibly expelled from the water phase and recovered as a solid. We suggest that this loss of stability is related to

the forces applied to the nano-emulsion during pumping, which are different from mechanical stirring. Based on these results, it was decided to proceed to crosslinking at a flow rate of 200 rpm as it allowed for a quick crosslinking without affecting the nano-emulsion stability. Because of the flow reactor cylindrical geometry, the microemulsion was alternately pushed by or against gravity at different segments, and local sedimentation may occur due to the gravity. We optimised the flow rate, which minimised compounding gravity and the hydrodynamic which could lead to sedimentation in the downwards flow segment of the tubing; meanwhile, the flow rate was sufficiently fast to counterbalance gravity as the suspension was pushed upwards. This methodology was further used to crosslink up to 50 g of nano-emulsion in less than 5 min.

3.6. Synthesis and characterisation of the microgels

Using the optimised flow-UV curing condition, CS microgels were obtained using the afore-described nano-emulsion templating method with a water phase consisting of 1 w:v% of CS-nbn-COOH in 2% AcOH, 0.1% of PI, and a designated amount of HS-DEG-SH crosslinker. The impact of three different surfactant compositions, corresponding to the optimised formulations, and four different crosslinker concentrations (calculated to vary the theoretical R_s from 1:4 to 1:1), were studied when the nano-emulsions were generated in both cyclohexane (**Figure 7**) and decane (**Figure S11**), comparing the sizes between the following five conditions: 1) microgels after they were washed and resuspended in water (brown); 2) microgels as crosslinked before washing (orange); 3) control nano-emulsions containing CS-nbn-COOH but not crosslinked (yellow); 4) control nano-emulsions with CS in the water phase (light green); and 5) control nano-emulsions with no added polymers to the water phase (dark green).

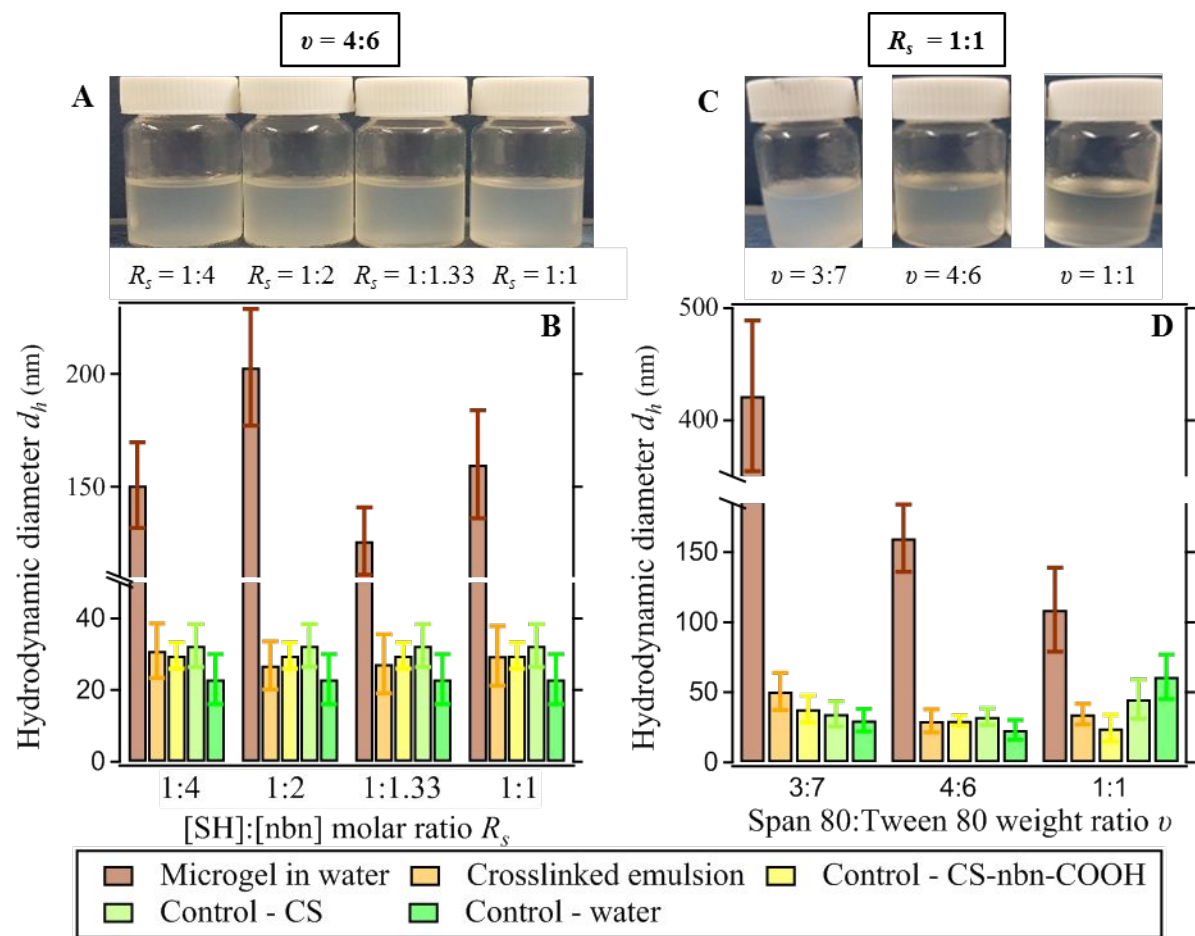


Figure 7. CS microgels made from the nano-emulsion templating method using cyclohexane as the oil phase. Photos of CS nano-emulsions generated from: **A)** a surfactant ratio S80:T80 $\nu = 4:6$ when varying the [SH]:[nbn] molar ratio R_s , from 1:1 to 1:4; **C)** different ratios ν of S80:T80 varying between 3:7 and 1:1 for $R_s = 1:1$. The corresponding hydrodynamic dimeters d_h , for **A)** and **C)**, measured by DLS, are shown respectively in **B)** and **D)**, for the isolated microgels in water (brown), the crosslinked nano-emulsions in cyclohexane (orange), and the control nano-emulsions containing uncrosslinked CS-nbn-COOH (yellow), native CS (light green) and no polymer (dark green) as the water phase.

For a given surfactant composition, the size of the microgel diameter did not vary significantly after crosslinking and was not affected by the [SH]:[nbn] molar ratio R_s (**Figure 7B**, orange bars),

thus demonstrating the robustness of the nano-emulsions. Once washed and resuspended in water, the microgels swelled and the diameter increased from $d_h \sim 40$ nm as obtained to $d_h \sim 120$ to 200 nm (**Figure 7B**, brown bars). The surfactant composition had a drastic impact on the size of the swollen microgel, with the largest value $d_h \sim 410$ nm obtained for $\nu = 3:7$, decreasing to $d_h \sim 110$ nm for $\nu = 1:1$ (**Figure 7D**). In contrast, when decane was used as the oil phase, the largest microgels obtained ($d_h \sim 190$ nm) corresponded to the smallest nano-emulsion template droplets (see **Figure S11**). This could be related to different degree of crosslinking accessible in the nano-reactors due to confinement, where smaller droplets could prevent the crosslinker to access all the reactive norbornene groups.

On the other hand, R_s had a small effect on the size of the isolated microgels, with d_h varying between 120 and 200 nm for the microgels obtained from the cyclohexane-templated nano-emulsion, and 140 and 240 nm for the decane template (**Figure 7B** and **Figure S11B**, respectively). TEM confirmed the formation of spherical objects for $R_s > 1:2$ with dry diameters $\sim 70 - 100$ nm, while a lower SH:nbn ratio ($R_s = 1:4$) gave a polydisperse mixture of spherical objects (**Figure 8**). All the microgels exhibited a zeta potential of around $\xi = +12$ mV, which is positive and lower than most previously reported CS-based microgels where $\xi \sim +50$ mV,⁴⁶ as expected by the introduction of carboxylic acid groups. ¹H NMR of the resulting microgels also showed traces of T80, which would impact on ξ , as well as unreacted norbornene (**Figure S12E**).

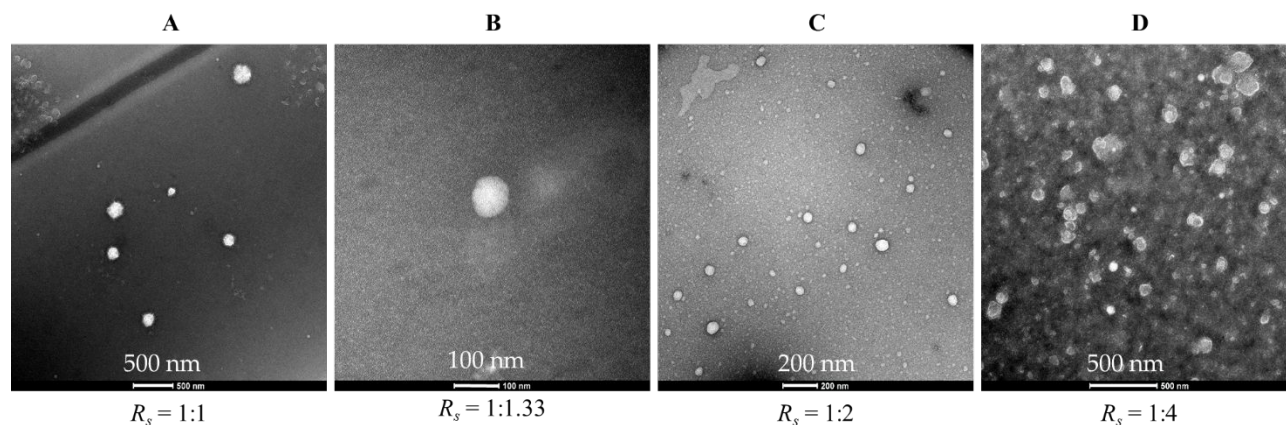


Figure 8. TEM of the CS-nbn-COOH microgels with R_s of: **A)** 1:4; **B)** 1:2; **C)** 1:1.33 and **D)** 1:1.

3.7. Microgel functionalisation

TEM images suggested that $R_s = 1:2$ was sufficient to provide spherical microgels, while ^1H NMR confirmed the presence of non-reacted norbornene groups, (**Figure S12E**). Furthermore, the relative sharpness of these alkene peaks compared to the crosslinked CS core strongly suggests that these moieties were located on the microgel surface and could therefore be accessed in a post-microgel synthesis step to design tailored, functionalised materials. This was investigated using tetrazine ligation, one of the fastest click chemistry reactions. Tetrazines typically weakly absorb at 515 nm, making it difficult to use absorbance to monitor the reaction efficiency.⁴⁷ Devaraj *et al.* reported fluorescent self-quenching tetrazines probes whose fluorescence increased up to 10 times after ligation.⁴⁸ A coumarin-functionalised tetrazine (Tet-Coum, **Figure 9**) was therefore synthesized and reacted with microgels. Within 2 min, a two-fold increase in fluorescence was observed, which increased up to three-fold and plateaued after 10 min of reaction time. This increase is consistent with the values reported by Devaraj *et al.* for a very similar probe to Tet-Coum.⁴⁸ This result supports the feasibility of the synthesis of more complex microgels, with decorations that could include cell targeting moieties⁴⁹ but also more expensive antibodies or proteins, thanks to the reliability of the tetrazine ligation.

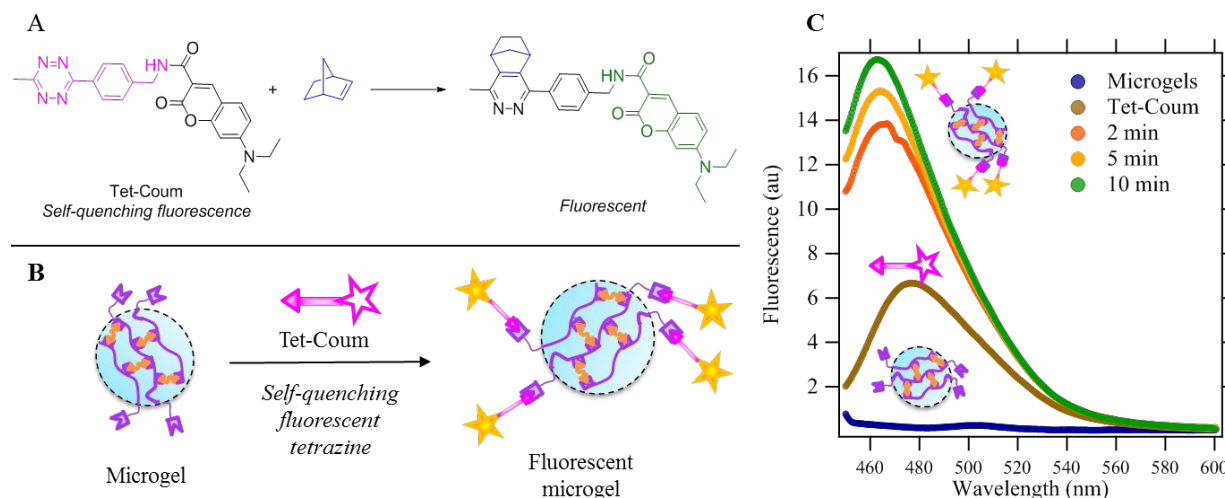


Figure 9. Functionalisation of microgels using tetrazine ligation. A) tetrazine ligation of Tet-Coum leading to a fluorescent molecule. B) Fluorescent-microgel synthesis using Tet-Coum. C) Fluorescence spectra of the microgels and Tet-Coum at different reaction time.

3.8. Microgel cytotoxicity

The toxicity of the microgels was assessed against HDF cell lines exposed to concentrations varied between 500 and 1 $\mu\text{g/mL}$ for 24 or 48 h using Alamar Blue (AB) to measure cell metabolic activity and Calcein AM to quantify cell viability. After 24 h both AB and Calcein AM measurements showed non-significant changes compared to control even at the highest investigated concentrations (**Figure 10A**) while the metabolic activity slightly decreased at high microgel concentration (500 and 250 $\mu\text{g/mL}$) after 48 h but remained comparable to the control at lower concentrations (**Figure 10B**). These preliminary results demonstrate the nontoxicity credentials of the microgels for their potential use in the biomedical area.

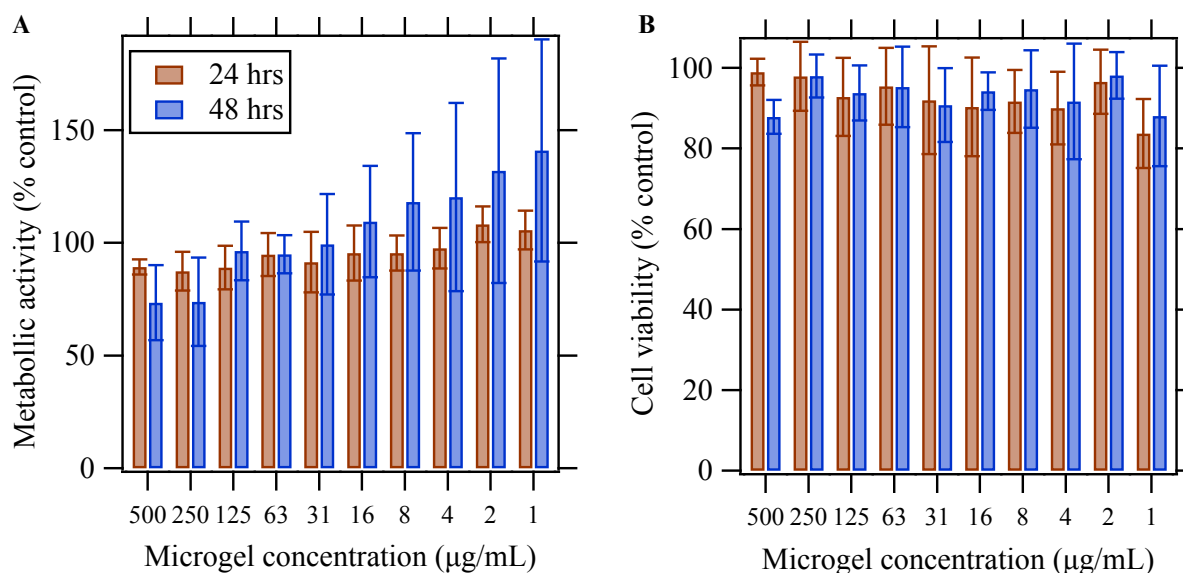


Figure 10. Toxicity data against HDF cell lines measured with A) AB (metabolic activity and B) Calcein AM (cell number). Results are expressed as a percentage normalised with respect to the control (untreated cells).

4. Conclusions

Soluble CS derivatives were successfully functionalised with norbornene through the formation of amide bonds using a coupling agent-free methodology by exploiting the ring-opening of carbic anhydride. The impact of various parameters on the substitution degree (DS) was studied, with the DS tuneable between 20 and 40 %. The designed polymers were successfully crosslinked through photoactivated thiol-ene chemistry using a domestic UV-A source and a cheap, commercially available thiolated PEG crosslinker; the use of such hydrogels as tissue engineering scaffolds is currently being investigated. Microgels of tailored size and degree of crosslinking were synthesized using an optimised low-energy, nano-emulsion-templated method in a flow reactor. Tuning of the nano-emulsion parameters allowed for the obtention of microgels of various sizes with pendant reactive groups, which could be accessed for late-stage functionalisation through

tetrazine ligation, as demonstrated by the grafting of a self-quenching fluorescent tetrazine probe, Tet-Coum. Finally, the described microgels presented non-significant toxicity against HDF cell lines and are therefore promising candidates as functional templates for biomedical applications, which is currently the object of further studies exploited.

ASSOCIATED CONTENT

Supporting Information.

Detailed experimental procedures and characterization data are available in the electronic supplementary information. The following files are available free of charge.

Chemical structure of the reagents used (Figure S1).

¹H NMR characterisations of CS and CS-nbn-CCOH including DS calculations (Figures S2 and S3).

Synthesis and characterisations of CS-nbn-H (Figure S4).

Experimental design experiments (Table S1).

Hydrogel characterisations, including photos (Figure S5) and ¹H NMR studies (Figure S6).

Control nano-emulsions of CS and CS-nbn in decane (Figure S7) and in cyclohexane (Figure S8).

Optimisation of the flow chemistry setup (Table S2).

Characterisation of microgel synthesised in decane (Figure S9).

¹H NMR characterisations of the microgels (Figure S10).

AUTHOR INFORMATION

Corresponding Authors:

* E-mail: m.c.galan@bristol.ac.uk; Phone: +44 (0) 117 928 7654

* E-mail: wuge.briscoe@bristol.ac.uk; Phone: +44 (0)117 3318256

Author Contributions

SM performed all the experiments and data analysis. The manuscript was written through contributions of all authors, who also contributed to the data analysis and interpretation. All authors have given approval to the final version of the manuscript.

Funding Sources

SM is supported by the Bristol Chemical Synthesis Centre for Doctoral Training (Engineering and Physical Science Research Council (EPSRC) EP/L015366/1). MCG acknowledges financial support by European Research Council (ERC-COG: 648239).

ACKNOWLEDGMENT

We thank Dr. Luke Elliott and Pr. Kevin Booker-Milburn for their help with the photochemistry, Pr. Craig Butts for helpful discussions on the NMRs, Paul Lehman for help with the NMR and Judith Mantell from the Wolfson Imaging Centre for TEM. We are indebted to the members of the Galan and Briscoe groups for helpful discussions on various aspects of synthesis and characterization.

REFERENCES

1. A. D. McNaught, A. W., IUPAC. Compendium of Chemical Terminology, 2nd ed. (the "Gold Book"). *Blackwell Scientific Publications* **1997**, 1807.
2. Oh, J. K.; Lee, D. I.; Park, J. M., Biopolymer-based microgels/nanogels for drug delivery applications. *Progress in Polymer Science* **2009**, *34* (12), 1261-1282.
3. Kateb, B.; Chiu, K.; Black, K. L.; Yamamoto, V.; Khalsa, B.; Ljubimova, J. Y.; Ding, H.; Patil, R.; Portilla-Arias, J. A.; Modo, M.; Moore, D. F.; Farahani, K.; Okun, M. S.; Prakash, N.; Neman, J.; Ahdoot, D.; Grundfest, W.; Nikzad, S.; Heiss, J. D., Nanoplatfoms for constructing new approaches to cancer treatment, imaging, and drug delivery: What should be the policy? *NeuroImage* **2011**, *54* (Supplement 1), S106-S124.
4. McClements, D. J., Designing biopolymer microgels to encapsulate, protect and deliver bioactive components: Physicochemical aspects. *Advances in Colloid and Interface Science* **2017**, *240*, 31-59.
5. Rami, L.; Malaise, S.; Delmond, S.; Fricain, J.-C.; Siadous, R.; Schlaubitz, S.; Laurichesse, E.; Amédée, J.; Montembault, A.; David, L.; Bordenave, L., Physicochemical

modulation of chitosan-based hydrogels induces different biological responses: Interest for tissue engineering. **2014**, *102* (10), 3666-3676.

6. Croisier, F.; Jérôme, C., Chitosan-based biomaterials for tissue engineering. *European Polymer Journal* **2013**, *49* (4), 780-792.

7. Bernkop-Schnürch, A.; Dünnhaupt, S., Chitosan-based drug delivery systems. *European Journal of Pharmaceutics and Biopharmaceutics* **2012**, *81* (3), 463-469.

8. Sahariah, P.; Måsson, M., Antimicrobial Chitosan and Chitosan Derivatives: A Review of the Structure–Activity Relationship. *Biomacromolecules* **2017**, *18* (11), 3846-3868.

9. Riegger, B. R.; Bäurer, B.; Mirzayeva, A.; Tovar, G. E. M.; Bach, M., A systematic approach of chitosan nanoparticle preparation via emulsion crosslinking as potential adsorbent in wastewater treatment. *Carbohydrate Polymers* **2018**, *180*, 46-54.

10. de Moraes Crizel, T.; de Oliveira Rios, A.; D. Alves, V.; Bandarra, N.; Moldão-Martins, M.; Hickmann Flôres, S., Active food packaging prepared with chitosan and olive pomace. *Food Hydrocolloids* **2018**, *74*, 139-150.

11. Lee, S.-M.; Liu, K.-H.; Liu, Y.-Y.; Chang, Y.-P.; Lin, C.-C.; Chen, Y.-S., Chitosonic(®) Acid as a Novel Cosmetic Ingredient: Evaluation of its Antimicrobial, Antioxidant and Hydration Activities. *Materials* **2013**, *6* (4), 1391-1402.

12. Saporito, F.; Sandri, G.; Rossi, S.; Bonferoni, M. C.; Riva, F.; Malavasi, L.; Caramella, C.; Ferrari, F., Freeze dried chitosan acetate dressings with glycosaminoglycans and traxenamic acid. *Carbohydrate Polymers* **2018**, *184*, 408-417.

13. Bhattarai, N.; Gunn, J.; Zhang, M., Chitosan-based hydrogels for controlled, localized drug delivery. *Adv Drug Deliv Rev* **2010**, *62* (1), 83-99.

14. Brunel, F.; Véron, L.; David, L.; Domard, A.; Delair, T., A Novel Synthesis of Chitosan Nanoparticles in Reverse Emulsion. *Langmuir* **2008**, *24* (20), 11370-11377.

15. Huang, Y.; Cai, Y.; Lapitsky, Y., Factors affecting the stability of chitosan/tripolyphosphate micro- and nanogels: resolving the opposing findings. *Journal of Materials Chemistry B* **2015**, *3* (29), 5957-5970.

16. Mazancová, P.; Némethová, V.; Treľová, D.; Kleščíková, L.; Lacík, I.; Rázga, F., Dissociation of chitosan/tripolyphosphate complexes into separate components upon pH elevation. *Carbohydrate Polymers* **2018**, *192*, 104-110.

17. Riederer, M. S.; Requist, B. D.; Payne, K. A.; Way, J. D.; Krebs, M. D., Injectable and microporous scaffold of densely-packed, growth factor-encapsulating chitosan microgels. *Carbohydrate Polymers* **2016**, *152*, 792-801.

18. Monteiro, O. A. C.; Airoidi, C., Some studies of crosslinking chitosan–glutaraldehyde interaction in a homogeneous system. *International Journal of Biological Macromolecules* **1999**, *26* (2), 119-128.

19. Szymańska, E.; Winnicka, K., Stability of Chitosan—A Challenge for Pharmaceutical and Biomedical Applications. *Marine Drugs* **2015**, *13* (4), 1819-1846.

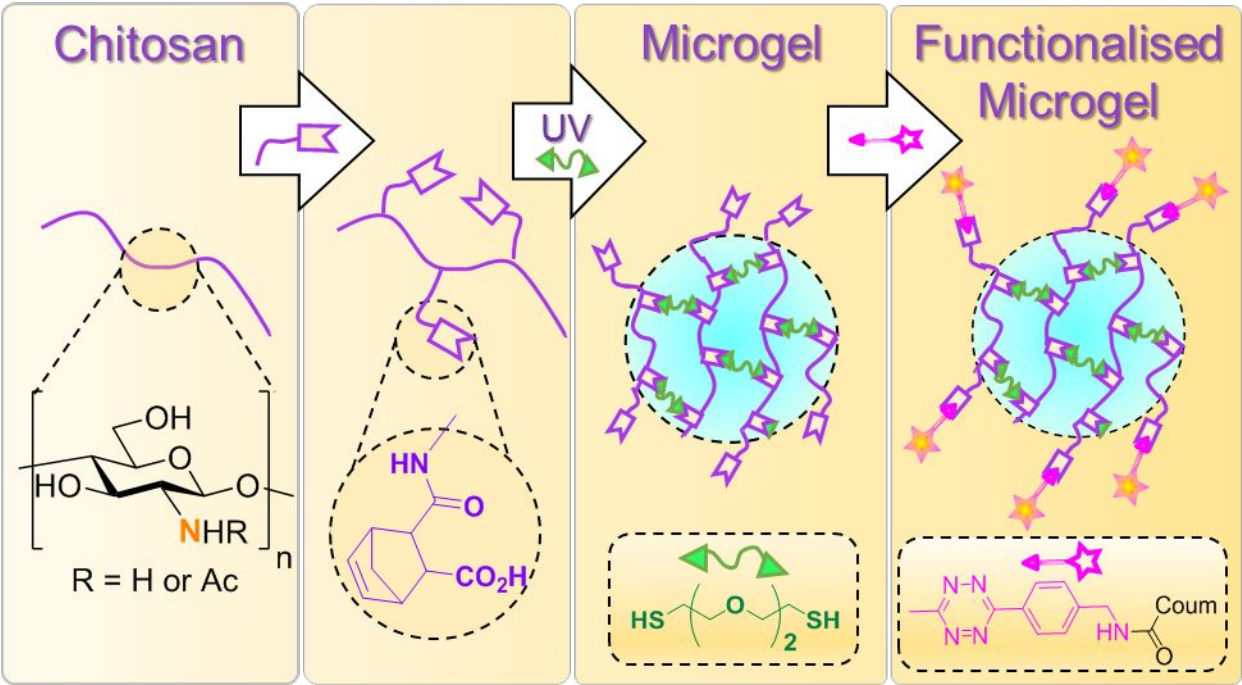
20. Jiang, Y.; Chen, J.; Deng, C.; Suuronen, E. J.; Zhong, Z., Click hydrogels, microgels and nanogels: Emerging platforms for drug delivery and tissue engineering. *Biomaterials* **2014**, *35* (18), 4969-4985.

21. Lin, C. C.; Ki, C. S.; Shih, H., Thiol-norbornene photo-click hydrogels for tissue engineering applications. *J Appl Polym Sci* **2015**, *132* (8), 41563.

22. Pei, M.; Mao, J.; Xu, W.; Zhou, Y.; Xiao, P., Photocrosslinkable chitosan hydrogels and their biomedical applications. *J. Polym. Sci. Part A: Polym. Chem.* **2019**, (doi:10.1002/pola.29305), 41563-41574.

23. Tomatsu, I.; Peng, K.; Kros, A., Photoresponsive hydrogels for biomedical applications. *Advanced Drug Delivery Reviews* **2011**, *63* (14), 1257-1266.
24. Devaraj, N. K.; Weissleder, R.; Hilderbrand, S. A., Tetrazine-Based Cycloadditions: Application to Pretargeted Live Cell Imaging. *Bioconjugate Chemistry* **2008**, *19* (12), 2297-2299.
25. Jivan, F.; Yegappan, R.; Pearce, H.; Carrow, J. K.; McShane, M.; Gaharwar, A. K.; Alge, D. L., Sequential Thiol–Ene and Tetrazine Click Reactions for the Polymerization and Functionalization of Hydrogel Microparticles. *Biomacromolecules* **2016**, *17* (11), 3516-3523.
26. Munoz, Z.; Shih, H.; Lin, C.-C., Gelatin hydrogels formed by orthogonal thiol-norbornene photochemistry for cell encapsulation. *Biomaterials Science* **2014**, *2* (8), 1063-1072.
27. Ooi, H. W.; Mota, C.; ten Cate, A. T.; Calore, A.; Moroni, L.; Baker, M. B., Thiol–Ene Alginate Hydrogels as Versatile Bioinks for Bioprinting. *Biomacromolecules* **2018**, *19* (8), 3390-3400.
28. McOscar, T. V. C.; Gramlich, W. M., Hydrogels from norbornene-functionalized carboxymethyl cellulose using a UV-initiated thiol-ene click reaction. *Cellulose* **2018**, *25* (11), 6531-6545.
29. Gramlich, W. M.; Kim, I. L.; Burdick, J. A., Synthesis and orthogonal photopatterning of hyaluronic acid hydrogels with thiol-norbornene chemistry. *Biomaterials* **2013**, *34* (38), 9803-11.
30. Zhou, Y.; Zhao, S.; Zhang, C.; Liang, K.; Li, J.; Yang, H.; Gu, S.; Bai, Z.; Ye, D.; Xu, W., Photopolymerized maleilated chitosan/thiol-terminated poly (vinyl alcohol) hydrogels as potential tissue engineering scaffolds. *Carbohydrate Polymers* **2018**, *184*, 383-389.
31. Jia, X.; Yeo, Y.; Clifton, R. J.; Jiao, T.; Kohane, D. S.; Kobler, J. B.; Zeitels, S. M.; Langer, R., Hyaluronic Acid-Based Microgels and Microgel Networks for Vocal Fold Regeneration. *Biomacromolecules* **2006**, *7* (12), 3336-3344.
32. Heller, D. A.; Levi, Y.; Pelet, J. M.; Doloff, J. C.; Wallas, J.; Pratt, G. W.; Jiang, S.; Sahay, G.; Schroeder, A.; Schroeder, J. E.; Chyan, Y.; Zurenko, C.; Querbes, W.; Manzano, M.; Kohane, D. S.; Langer, R.; Anderson, D. G., Modular ‘Click-in-Emulsion’ Bone-Targeted Nanogels. *Advanced Materials* **2013**, *25* (10), 1449-1454.
33. Gupta, A.; Badruddoza, A. Z. M.; Doyle, P. S., A General Route for Nanoemulsion Synthesis Using Low-Energy Methods at Constant Temperature. *Langmuir* **2017**, *33* (28), 7118-7123.
34. Hook, B. D. A.; Dohle, W.; Hirst, P. R.; Pickworth, M.; Berry, M. B.; Booker-Milburn, K. I., A Practical Flow Reactor for Continuous Organic Photochemistry. *The Journal of Organic Chemistry* **2005**, *70* (19), 7558-7564.
35. Yu, L. M. Y.; Kazazian, K.; Shoichet, M. S., Peptide surface modification of methacrylamide chitosan for neural tissue engineering applications. **2007**, *82A* (1), 243-255.
36. Perera, M. M.; Ayres, N., Gelatin based dynamic hydrogels via thiol-norbornene reactions. *Polymer Chemistry* **2017**, *8* (44), 6741-6749.
37. Gramlich, W. M.; Kim, I. L.; Burdick, J. A., Synthesis and orthogonal photopatterning of hyaluronic acid hydrogels with thiol-norbornene chemistry. *Biomaterials* **2013**, *34* (38), 9803-9811.
38. Fraser, A. K.; Ki, C. S.; Lin, C.-C., PEG-Based Microgels Formed by Visible-Light-Mediated Thiol-Ene Photo-Click Reactions. *Macromolecular Chemistry and Physics* **2014**, *215* (6), 507-515.
39. Lee, S.; Park, Y. H.; Ki, C. S., Fabrication of PEG–carboxymethylcellulose hydrogel by thiol-norbornene photo-click chemistry. *International Journal of Biological Macromolecules* **2016**, *83*, 1-8.

40. Mergy, J.; Fournier, A.; Hachet, E.; Auzély-Velty, R., Modification of polysaccharides via thiol-ene chemistry: A versatile route to functional biomaterials. *Journal of Polymer Science Part A: Polymer Chemistry* **2012**, *50* (19), 4019-4028.
41. Hachet, E.; Sereni, N.; Pignot-Paintrand, I.; Ravaine, V.; Szarpak-Jankowska, A.; Auzély-Velty, R., Thiol-ene clickable hyaluronans: From macro-to nanogels. *Journal of Colloid and Interface Science* **2014**, *419*, 52-55.
42. Davies, R.; Graham, D.; Vincent, B., *Water-cyclohexane-“Span 80”-“Tween 80” systems: Solution properties and water/oil emulsion formation*. 1987; Vol. 116, p 88-99.
43. Gupta, A.; Eral, H. B.; Hatton, T. A.; Doyle, P. S., Controlling and predicting droplet size of nanoemulsions: scaling relations with experimental validation. *Soft Matter* **2016**, *12* (5), 1452-1458.
44. Gupta, A.; Eral, H. B.; Hatton, T. A.; Doyle, P. S., Nanoemulsions: formation, properties and applications. *Soft Matter* **2016**, *12* (11), 2826-2841.
45. Su, H.; Jia, Q.; Shan, S., Synthesis and characterization of Schiff base contained dextran microgels in water-in-oil inverse microemulsion. *Carbohydrate Polymers* **2016**, *152*, 156-162.
46. Goycoolea, F. M.; Lollo, G.; Remuñán-López, C.; Quaglia, F.; Alonso, M. J., Chitosan-Alginate Blended Nanoparticles as Carriers for the Transmucosal Delivery of Macromolecules. *Biomacromolecules* **2009**, *10* (7), 1736-1743.
47. Oliveira, B. L.; Guo, Z.; Bernardes, G. J. L., Inverse electron demand Diels–Alder reactions in chemical biology. *Chemical Society Reviews* **2017**, *46* (16), 4895-4950.
48. Devaraj, N. K.; Hilderbrand, S.; Upadhyay, R.; Mazitschek, R.; Weissleder, R., Bioorthogonal Turn-On Probes for Imaging Small Molecules inside Living Cells. **2010**, *49* (16), 2869-2872.
49. Praphakar, R. A.; Shakila, H.; Azger Dusthacker, V. N.; Munusamy, M. A.; Kumar, S.; Rajan, M., A mannose-conjugated multi-layered polymeric nanocarrier system for controlled and targeted release on alveolar macrophages. *Polymer Chemistry* **2018**, *9* (5), 656-667.



TOC Graphic.